17th World Conference on Earthquake Engineering, 17WCEE

Sendai, Japan - September 13th to 18th 2020

ON THE EFFECTS OF THE VERTICAL COMPONENT ON THE SEISMIC RESPONSE OF URM BUILDINGS

S. Lagomarsino[(1)], S. Degli Abbati [(2)], S. Cattari [(3)]

[(1)] *Full professor, University of Genoa, sergio.lagomarsino@unige.it*
[(2)] *Post-doc fellow, University of Genoa, stefania.degliabbati@unige.it*
[(3)] *Associate Professor, University of Genoa, serena.cattari@unige.it*

Abstract

The vertical component of the ground motion is usually ignored in the seismic assessment of existing building, even if recently a high vertical component of the seismic acceleration has been recorded in some earthquakes (*e.g.* the 2012 Emilian earthquake) highlighting possible critical effects for existing buildings. At present, the state-of-art on possible approaches to take into consideration the effects of the vertical ground motion on the building performance is very poor, but at the same time, many engineers are wondering how to deal with this issue. Within this context, the paper investigates the influence of applying a single or two horizontal components of the ground motion and also considering the vertical component on the nonlinear dynamic response of UnReinforced Masonry (URM) structures. In particular, NonLinear Dynamic Analyses (NLDA) have been performed on a case-study, representative of 3-storeys brick masonry building characterized by stiff horizontal diaphragms. The analyses have been performed with the software Tremuri, thus referring to the equivalent frame modeling approach, and using two different accelerograms: the Mirandola record from 29th May 2012 Emilian earthquake; and the Norcia record of 30th October 2016 from the 2016 Central Italy earthquake. Different analyses have been performed, alternatively applying: i) only the E-W component; ii) only the N-S components; iii) both the horizontal components; iv) the whole three components. The results of these analyses are then compared, referring to different Engineering Demand Parameters (EDPs) for interpreting the potential effects on the structural response: the maximum top displacement (selected in order to highlight the vertical ground motion effect at a *"global scale"*); the axial force variation and the damage pattern recorded in some piers (selected in order to highlight the vertical ground motion effect at a *"local scale"*). Finally, the results of the NLDA have been compared with those provided by NonLinear Static Analyses (NLSA), by decreasing the vertical gravity forces according to an assumed triangular vertical modal shape along with the pushover analysis.

Keywords: vertical component; seismic response; masonry; nonlinear dynamic analysis; equivalent static approach

1. Introduction

The seismic assessment of existing buildings usually refers only to the horizontal components of the input motion. In fact, except for effects of local amplification phenomena, ordinary buildings are more vulnerable to the horizontal components of the seismic motion. However, in the recent past, some high vertical components of the seismic acceleration have been recorded (*e.g.* the 2012 Emilian earthquake) and various authors ([1],[2]) highlighted the possible negative effects of the Vertical Ground Motion (VGM) to explain some observed damage mechanisms in UnReinforced Masonry (URM) buildings. Moreover, the evaluation of VGM effect on existing masonry buildings can be interesting as their vertical frequencies could be resonant with the high frequencies of the vertical seismic input [3].

At present, the state-of-art on possible approaches to take into consideration the effects of the VGM on the building performance is very poor. Past studies deepened the effects of the vertical component mostly on Reinforced Concrete (RC) structures ([4], [5]), finding out that the vertical component determines an important variation of the axial forces in structures placed near the epicenter with a source-to-site distance lower than 30 km. Moreover, other research works ([6], [7]) analyzed different RC structural models through NonLinear Dynamic Analyses (NLDA) and noticed that: axially stiff structures (i.e. with vertical periods included in the 0.05-0.15 s range) were subjected to a significant dynamic amplification due to the vertical excitation; and shear failures can occur in the upper floors, where the compression axial forces due to the gravity loads may be counterbalanced by the effects of the VGM that induce tensile axial forces (thus reducing the walls shear capacity). More recently, some authors investigated the effects of the ground motion vertical effects on URM structures, as well. Di Michele et al. 2019 [3] performed NLDA with a selection of natural ground motion records characterized by different source-to-site distance, fault rupture type, ground category and moment magnitude and they found out a clear correlation among the velocity spectrum intensity, the considered Engineering Demand Parameters (EDPs) (i.e. the horizontal and vertical displacements, and the axial and shear forces) and the incidence of the source-to-site distance on the vertical component effects. Their results highlighted that the vertical component can generate tensile forces in the masonry piers (especially where the gravity loads are small) for records with low source-to-site distance and high moment magnitude, with potential reduction of the flexural and shear capacity of piers. Liberatore et al. 2019 [8] analyzed the effects of the coseismic ground vertical motion on masonry constructions during the earthquakes that hit Central Italy in 2016, since they observed that the most significant damage was recorded in areas that underwent subsidence, while in those closer to the epicenter, but coseismically uplifted, the occurred damage was lower. They performed numerical simulations on a URM structure considering a cohesive-frictional unit-mortar interface to understand the effect of vertical acceleration and by analyzing the resulting variation of friction forces between units and mortar. Results highlighted that the vertical component effects are more significant in those structures with small cohesion, determining more extensive failures, due to the greater high-frequency content of the vertical ground acceleration (compared with horizontal displacement) that determines, during a single sliding along a mortar joint, several cycles of vertical stress at the interface. Mariani et al. (2018) [9] investigated the negative effects of the vertical ground motion on existing masonry buildings, attributing to it, among the different aspects, a fundamental contribution to the loss of ductility and consequent collapse. As a consequence, they promoted the necessity to always consider the VGM since relevant in both far and near-to-the-source areas [10]. Despite the increasing attention on this topic, an unanimous approach to treat it is still lacking and also professional engineers are wondering how to deal with this issue.

Within this context, the paper investigates the influence of applying a single or two horizontal components of the ground motion and also considering the vertical component on the nonlinear dynamic response of UnReinforced Masonry (URM) structures. In particular, NLDA have been performed on a case-study representative of 3-storeys brick masonry building characterized by stiff horizontal diaphragms. The building was alternatively studied in two different configurations, obtained by varying the distribution of masses and stiffness in plan. The analyses have been performed with the software Tremuri [11], that works

according to the equivalent frame modeling approach, and using two different accelerograms recorded in some recent Italian earthquakes (Emilia 2012 and Central Italy 2016/2017).

With the aim of investigating the effects of the seismic motion vertical component on the structural response of URM buildings, different analyses have been performed, alternatively applying: i) only the E-W component; ii) only the N-S components; iii) both the horizontal components; iv) the whole three components. Finally, the results of the NLDA have been compared with those provided by some NonLinear Static Analyses (NLSA) performed by decreasing the vertical gravity forces according to an assumed triangular vertical modal shape along with the pushover analysis. This is an approximate way to include the vertical component also in the static approach that has been originally proposed in [12], [13] and herein tested for verify its reliability in comparison with the dynamic one.

2. Case-study description

The case-study building analyzed in the paper is an URM building with brick masonry and stiff horizontal diaphragms. The structure has 3 stories (total height equal to 10.8 m) and a rectangular plan (14 x 10 m). The structural model has been set through the software Tremuri [11], thus referring to the equivalent frame modeling approach. According to this approach, each wall is discretized by a set of masonry panels (piers and spandrels), in which the non-linear response is concentrated, connected by a rigid area (nodes). Only the in-plane response of masonry walls is considered. The complete 3D model is obtained by introducing also floor elements, which are modeled as orthotropic membrane finite elements characterized by limited stiffness. Fig. 1 illustrates the plan and the mesh of the perimeter walls. The load-bearing structure consists of eight walls; four of them are in the x-direction (Walls 1, 3, 7 and 8) while the other four are in the y-direction (Walls 2, 4, 5 and 6). Moreover, in order to have some additional information, a further configuration (hereafter named "Regular") has been analyzed, obtained by varying the distribution of masses and stiffness in plan.

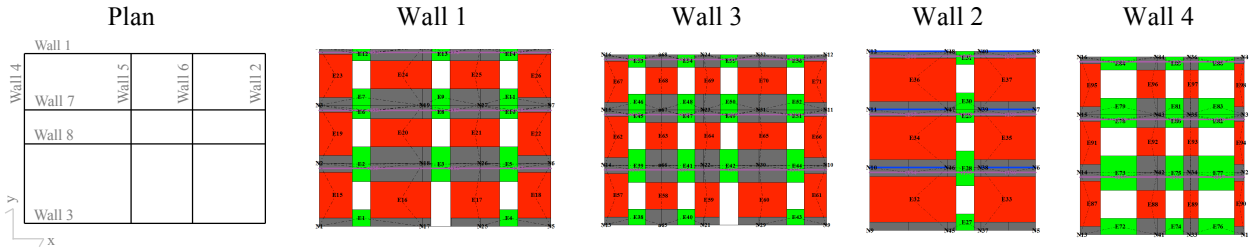

Fig. 1 – Plan and mesh of the perimeter walls

The constitutive law adopted for describing the nonlinear response of masonry panels is the piecewise-linear one, implemented in Tremuri [14]. This constitutive law (Fig. 2) simulates the nonlinear response until very severe damage levels (from 1 to 5) through progressive stiffness and strength degradation (defined in terms of residual strength β_i) in correspondence of assigned values of drift (θ_i). The hysteretic response is formulated through a phenomenological approach that, thanks to a proper setting of specific coefficients (c_i with i=1,…,4), allows easily capturing the differences among the various possible failure modes (flexural, shear or hybrid) and the different response of piers and spandrels. Concerning the necessary parameters to be defined, the used strength mechanical parameters are presented in Table 1, starting from the reference ones proposed in the Italian Technical Code [15].

Table 1 – Mechanical parameters of the model

	$E^{(1)}$ [MPa]	$G^{(1)}$ [MPa]	w [kN/m^3]	f_m [N/cm^2]	τ_0 [N/cm^2]
Solid brick and lime mortar	1500	500	18	280	10
(1) Un-cracked values; w: average specific weight; f_m: compressive strength; τ_0: shear strength					

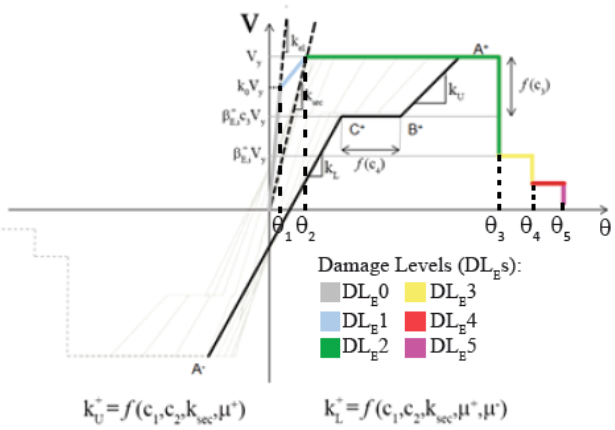

a.

Piers/ Spandrels	SHEAR (S)			
	Backbone curve		Hysteretic response	
	θ_i [%]	β_i [%]	c_1	0.8/0.2
DL3	0.30/0.20	0.7/0.6	c_2	0.8/0
DL4	0.50/0.60	0.4/0.6	c_3	0/0.3
DL5	0.70/2.0	0/0		
Piers/ Spandrels	FLEXURAL (F)			
	θ_i [%]	β_i [%]	c_1	0.9/0.2
DL3	0.60/0.20	1	c_2	0.8/0
DL4	1.0/0.60	0.85/0.60	c_3	0.6/0.3
DL5	1.5/2.0	0/0	c_4	0.5/0.8

b.

Fig. 2 – Piecewise-linear constitutive law (a) and parameters adopted for masonry panels in the NL field (b)

Table 2 shows the first two modes of the examined case-study (which are respectively in the y and x-directions) and some other modes from 16 to 24, which are characterized by a vertical participation mass, particularly for mode 21 (with M_z=34%). As one can see, the case-study is characterized by a first period in the y-direction equal to 0.275 s and in the x-direction equal to 0.219 s, while the mode activating the most significant mass percent in the z-direction is characterized by a period of 0.058 s.

Table 2 – Results of the modal analysis (elastic mechanical parameters)

Mode	**1**	**2**	**16**	**21**	**22**	**24**
T [s]	0.275	0.219	0.063	0.058	0.056	0.054
M_x [%]	0	66	1	0	0	0
M_y [%]	66	0	1	0	0	0
M_z [%]	0	0	5	34	18	5

3. Used ground motions

Two records have been adopted for performing the NLDA: the Mirandola (MRN) record from 29th May 2012 Emilian earthquake and one record from the 2016 Central Italy earthquake (the Norcia – NRC - record from 30th October 2016). They have been selected since they present very different features (as better described later), even if both are characterized by a small source-to-site distance (< 10 km), thus the effects of the vertical component are expected to be more evident ([3], [5], [16]).

Table 3 summarizes some data of the records selected in terms of: epicentral distance (d); Peak Ground Accelerations (PGA) of the two H components (PGA_{EW} and PGA_{NS}) and of the V one (PGA_V); spectral acceleration of the H components of the records ($S_{a,EW}$ and $S_{a,NS}$) calculated as the integral in correspondence of a range of periods representative of the dynamic response in the x and y directions (0.24s<T<0.5s); spectral acceleration of the V component of the records calculated as the integral in the same range of periods ($S_{a,V}$) or in correspondence of a range of periods representative of the dynamic response in the z-direction ($S_{a,V'}$, 0.04s<T<0.1s); ratio between vertical V and horizontal H PGA ($PGA_{V/H}$) and spectral acceleration in correspondence of the above-mentioned range of periods ($S_{a,V/H}$, $S_{a,V'/H}$). In these latter cases, the H component was obtained as geometric mean of the two horizontal components, since this one represents the most commonly used parameters when single horizontal spectrum is used [17]. Concerning the definition of the range of periods representative of the structural dynamic response, it has to

be pointed out that it has been defined starting from the results of the modal analysis (§2) and assuming a period elongation in the nonlinear fields, due to the occurrence of some structural damage.

Table 3 – Brief data of the records selected for the analysis

Record	d [km]	PGA_{EW} [m/s^2]	PGA_{NS} [m/s^2]	PGA_{V} [m/s^2]	$S_{a,EW}$ [m/s^2]	$S_{a,NS}$ [m/s^2]	$S_{a,V'}$ [m/s^2]	$S_{a,V}$ [m/s^2]	$PGA_{V/H}$ [-]	$S_a(T)_{V'/H}$ [-]	$S_a(T)_{V/H}$ [-]
MRN	8	2.205	2.902	8.715	4.61	6.53	25.72	3.38	3.45	4.69	0.62
NRC	5	4.787	3.645	3.682	13.07	8.34	8.97	6.66	0.88	0.86	0.64

Fig. 3 shows the comparison between the three components of the records used in the analyses (a), in a significant time window of the records, the corresponding acceleration spectra (b) and the ratio between vertical (V) and horizontal (H) spectra calculated for each period compared between the two events.

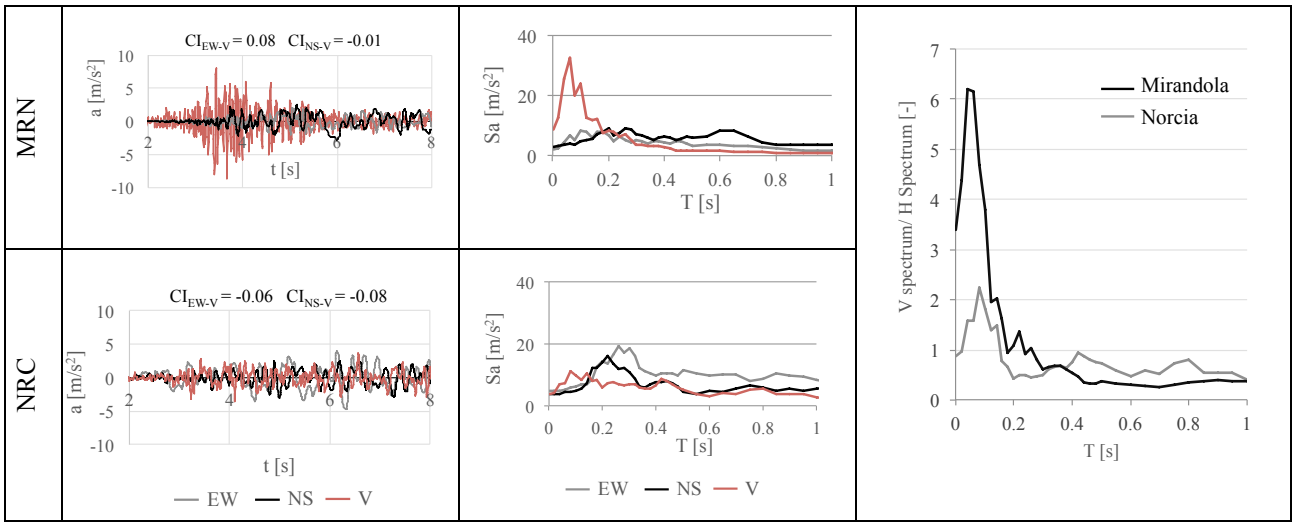

a. b. c.

Fig. 3 –Records used in the analyses (a) and corresponding acceleration spectra (b); ratios between vertical (V) and horizontal (H) spectra (c)

As one can see from Table 3 and Fig. 3, the Mirandola record is characterized by a V component with high frequency and that comes before the H ones, as often happen for the P waves that precede the S ones. This is also clear comparing $S_{a,V'}$ with $S_{a,V}$. The first value is significantly higher than the second one; this indicates that the V spectrum peak is concentrated in correspondence of periods lower than the ones characterizing the dynamic response in x and y direction, while in this latter range of periods the integral of the V spectrum is quite similar to the integral of the H spectrum. Furthermore, in Mirandola record, the PGA_V is significantly higher than the PGA_H. Instead, the Norcia record has a V component that reaches the maximum values at the time with the H ones and characterized by the same intensity. Moreover, from Fig. 3c it is possible to see that the effects of the vertical component are more significant in the range of periods T=0-0.2 s, that is lower than the range of periods which characterize the dynamic response in the x and y directions of the examined structure (0.24s<T<0.5s), but that is also close to the one connected to the dynamic response in the z direction (0.04s<T<0.1s). In particular, the Mirandola record has in this range a very important ratio V/H ratio (close to 6). Finally, for the Correlation Index (CI) calculated between the H and V components of each record and shown in Fig. 3a, one can see that the three components of the accelerograms are not correlated (since the CI is close to zero).

4. Analyses and results

4.1 Nonlinear dynamic analyses

Fig. 4a-b presents the comparison between the dynamic curve V-d obtained from the NLDA alternatively applying only the horizontal components of each record (the N-S in the x-direction and the E-W in the y-direction) and all the three components, including the vertical one in the z direction. For sake of example, only the curves in the x direction are plotted in the figures. The dynamic hysteretic cycles are compared with the pushover curve in the x-direction obtained applying a uniform load distribution; results refer to the "Irregular" configuration. From this comparison, one can see that these records induced a significant nonlinear response in the structure. Moreover, Fig. 4c-d compares the displacements time history in the x-direction, induced by applying only one H component (alternatively the N-S in the x direction or the E-W in the y direction – grey curves), both the two H components (black curve) and the whole three components (red curve) of the selected records. A more systematic comparison among the maximum displacements obtained (in x and y directions) is illustrated in Table 4. In the table, in order to have some additional information, the results obtained from the "Regular" configuration (described at §2) have been presented as well.

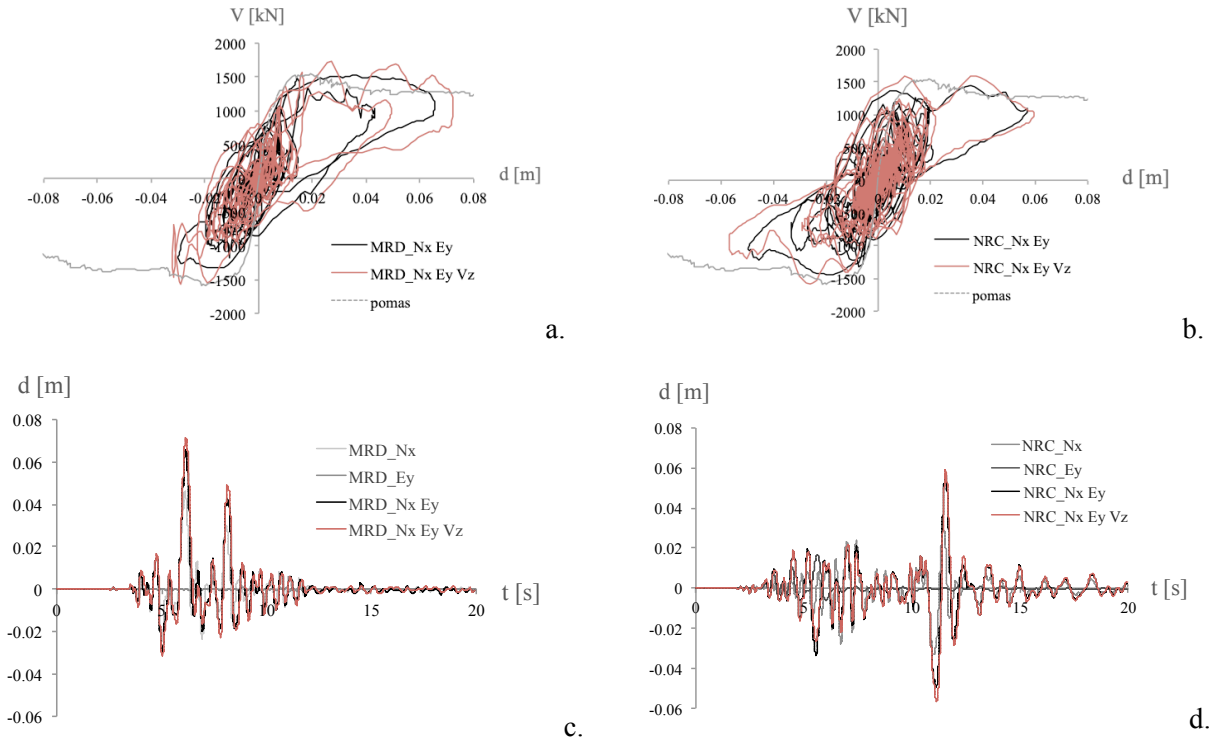

Fig. 4 – NL hysteretic response applying only the H (black graphs) or H+V (red graphs) components of the MRD (a) and NRC (b) records *vs* pushover curve (uniform distribution); displacements time history obtained applying only one, two or three components of the MRD (c) and NRC (d) records

As one can see from Fig. 4c-d, the vertical component of the record induces in the structure an increase of the peak displacement. However, it is interesting to notice from Table 4 that in general the most significant increase of displacement is due to the two H components (with a maximum increase of Δ_H=41% in the x direction for the MRD record and of Δ_H=71% for the NRC record), while the additional V component determined only a slight further increase Δ_V. However, one can notice from these results that the maximum displacement values as function of the considered components are quite random and that there is

not a more systematic trend by considering the "Regular" configuration of the case-study. For example, for the NRC record in the y-direction and for the case-study analyzed in the "Regular" configuration, the maximum displacement induced considering the H+V components is lower than the corresponding one obtained applying only the H components. These results highlight also that probably the maximum top displacement is not the most effective Engineering Demand Parameter (EDP) to be considered for the examined case-study to evaluate the VGM effect on the response of URM structures.

Table 4 – Maximum top displacements in the x and y directions and increase percent due to two (Δ_H) or three (Δ_V) components

		x-direction					y-direction				
Records	**Configuration**	**Nx [cm]**	**NxEy [cm]**	**NxEyVz [cm]**	**Δ_H [%]**	**Δ_V [%]**	**Ey [cm]**	**NxEy [cm]**	**NxEyVz [cm]**	**Δ_H [%]**	**Δ_V [%]**
MRN	Irregular	4.6	6.6	7.2	41	10	1.8	2.0	2.5	13	21
	Regular	4.2	6.4	6.7	53	6	1.9	2.6	2.6	33	1
NRC	Irregular	3.4	5.7	6.0	71	4	13.7	12.9	14.5	-6	12
	Regular	3.2	3.4	3.7	9	9	13.0	15.4	10.8	19	-30

4.2 Effects of the vertical component on the axial force variation

In order to deepen the VGM effect at a *"local scale"*, the response of some panels have been investigated through the definition of their strength domain. Fig. 5 shows the V-N (shear – axial force) interaction diagrams for piers n. 136, 144 (placed respectively at the first and third level on one side of wall 7 – see Fig. 1) and pier n. 58 (placed in the central part of wall 3 at the first level). The red and black clouds of points represent V-N pairs for the above-mentioned piers at each time step of the MRD ground motion, obtained by alternatively applying both the H components (black line) and the three components (red line).

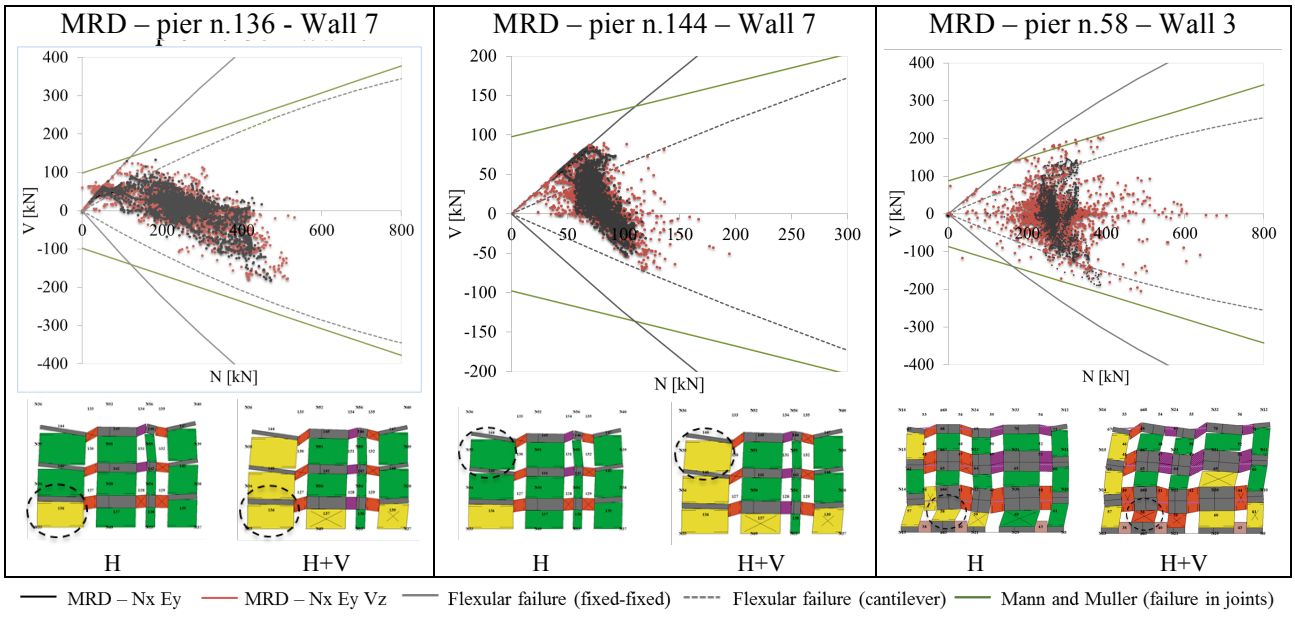

Fig. 5 – V-N interaction diagrams for piers n. 136, 144 and 58 at each time step of MRD ground motion and comparison of the damage pattern at the end of the analysis by applying both the H components (H) and the three components (H+V)

In particular, in Fig. 5 the whole domain is presented considering: in the case of shear failure, the Mann and Muller criterion with failure in the mortar joints [18] (in green in the figure); while in the case of

flexural failure, two different possibilities as a function of the cantilever (grey dotted line) or fixed-fixed (grey continuous line) static scheme. Moreover, Fig. 5 presents the comparison of the damage pattern at the end of the analysis considering (H+V) or neglecting (H) the vertical components of the record. From Fig. 5 it is possible to observe a different behavior of the two piers n. 136 and 144, placed at the extremity of wall 7, and pier n. 58, placed instead in the central part of wall 3. In pier 136 (that is at the first level), it is interesting to observe a variation of the axial force due to the horizontal components of the seismic action that induced compression at one extremity of the wall and decompression on the opposite one. At the top level of the building, an additional contribution of variation of axial force is due to the vertical component, which is more relevant there as a result of the modal deformed shape of the vertical modes that are about triangular, thus higher at the high level. This is clear by observing the V-N interaction diagram for pier 144. Instead, in piers placed at the centre of the walls (as pier n. 58 in the wall 3) there is not a variation of the axial force due to the H components, thus the variation of the axial force that one can appreciated from the analyses is only due to the vertical component. In this latter case, the H+V analysis show larger variations of N in pier 58 than the H analysis.

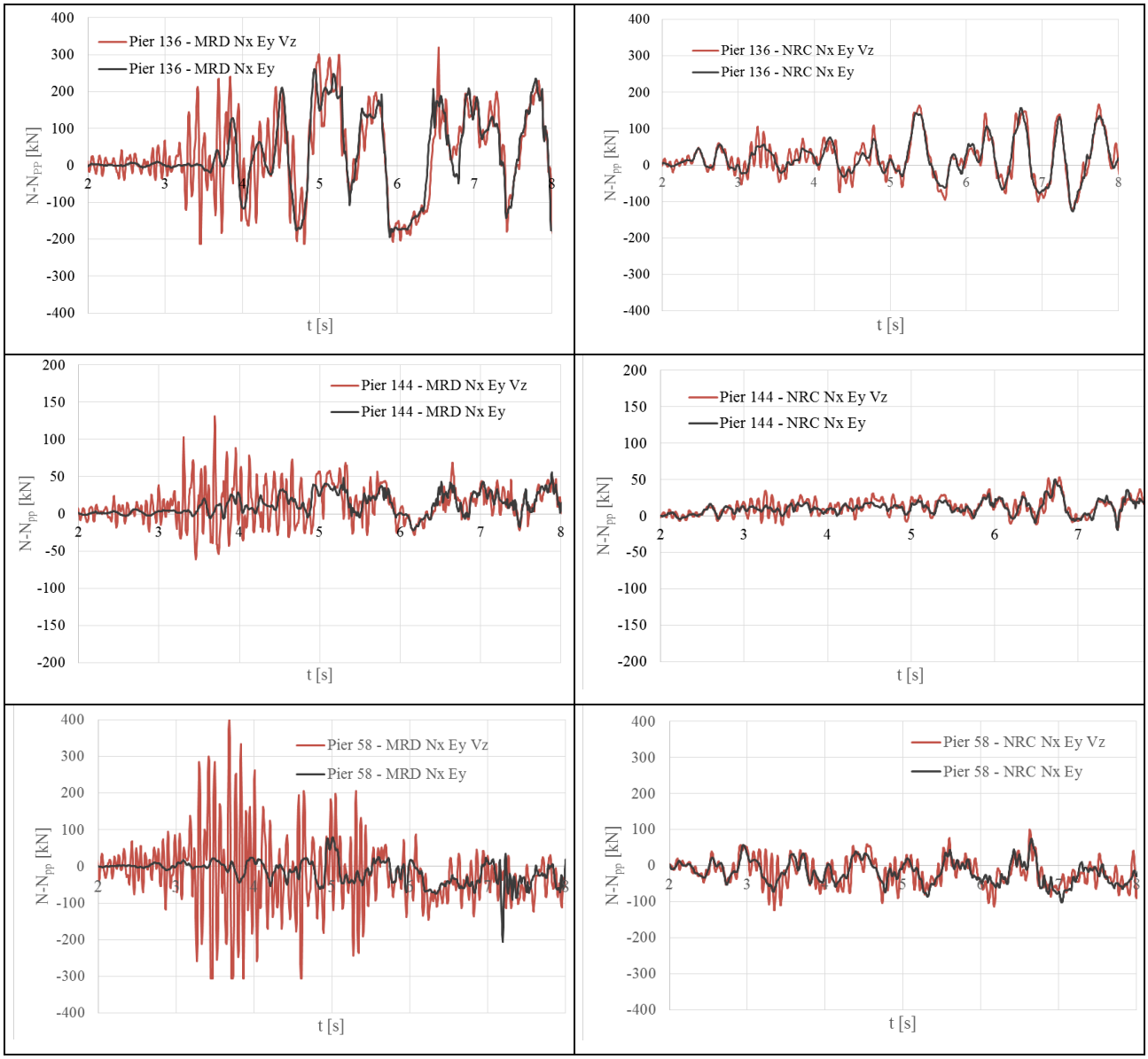

Fig. 6 – Variation of the axial force (minus N due to gravity load) for MRD and NRC records *vs* time obtained analysis by applying both the H components (H) and the three components (H+V)

Fig. 6 compares the results in terms of the time history of the variation of the axial force with respect to the initial value due to gravity load ($N-N_{PP}$), for the same piers but in the analyses performed with MRD and NRC records, again alternatively considering or neglecting the V component. From this figure, it is interesting to observe that the NRC record seems not to convey the VGM effect, either for the central piers or for the extremity ones. From these results, it seems that the VGM effect is more relevant for records with a significant vertical PGA, even if the V component is not correlated with the H components.

5. Comparison between NLDA and NLSA

Finally, the results of the NLDA have been compared with those provided by the NLSA performed by decreasing the vertical gravity forces according to an assumed triangular vertical modal shape along with the pushover analysis. In particular, since the state-of-art on the possible approaches to take into consideration the vertical ground motion is very poor ([12], [13]), the value of the maximum reduction at the level z=H (with H the total height of the structure) has been calculated, considering any node *i* at the level z_i=H, as:

$$\frac{\Delta_g}{g} = \frac{F_i}{W_i} = 0.405 \cdot S \cdot F_0 \cdot \lambda \cdot \left(\frac{a_g}{g}\right)^{1.5} \cdot \frac{H \cdot W_{TOT}}{\sum_j z_j \cdot W_j} \quad (1)$$

where S is the site coefficient, F_0 is the spectral amplification factor (both defined at §3.2.3.2 of NTC 2018 [19]), λ is a coefficient equal to 0.85 for 3-story or higher building, W_{TOT} is the total weight of the structure, z_j and W_j are respectively the level and weight of the j^{th} mass (defined at §7.3.3.2 of NTC 2018 [19]). In particular, the ratio $\frac{H \cdot W_{TOT}}{\sum_j z_j \cdot W_j}$ has to be calculated from the mass matrix of the structural model, known the levels of the nodes. For masses uniformly distribued, as in the examined case, it is equal to 1.5 (it is higher than 1.5 if the masses are concentrated at the lowest levels, while it is included in the range 1-1.5 if they are concentrated at the top levels).

Eq. (1) has been defined following the prescriptions provided by Italian Technical Code for the linear static analysis (Eq. 7.3.7 of §7.3.3.2 of NTC 2018 [19]), by substituting the value of the maximum horizontal spectrum calculated at the structural fundamental period with the corresponding vertical one ($S_{v,max}$) and evaluating the 30%, consistently with the normative recommendations, since the vertical component is applied instantaneously. $S_{v,max}$ has been instead calculated as in Eq. (2), following the prescriptions of [19] at §3.2.3.2.2 and considering a 5% damping (thus, η=1), being F_v a coefficient that quantify the maximum spectral amplification, in terms of maximum horizontal acceleration on the site a_g on a rigid horizontal reference site.

$$S_{v,\max} = S_{ve}(T = T_B) = a_g \cdot S \cdot F_v = 1.35 \cdot S \cdot g \cdot F_0 \cdot \left(\frac{a_g}{g}\right)^{1.5} \quad (2)$$

Table 5 shows the acceleration decrease by varying the horizontal peak acceleration considering for the examined case S=1, F_0=2.5, $\frac{H \cdot W_{TOT}}{\sum_j z_j \cdot W_j}$ =1.5 and λ=0.85.

Table 5 – Acceleration decrease Δg/g by varying the value of a_g/g

a_g/g	0.05	0.15	0.25	0.35
Δg/g	0.014	0.075	0.161	0.267

Fig. 7 illustrates the comparison between the NLD hysteretic cycles obtained with the NRC record in the x-direction (by applying both the H components of the H+V components) and the pushover analyses from the NLSA performed by assuming a uniform load pattern (red curve) and alternatively decreasing the vertical gravity forces of 10% (blue curve) and 30% (green curve). In particular, since the value of the spectral acceleration of the V component of the NRC record calculated in correspondence of a range of periods representative of the dynamic response in the z-direction $S_{a,V}(T_z)$ is equal to about 1 g (Fig. 3b) and since the Italian Technical Code prescribes to consider a 30% of this value, the pushover analysis which aimed to simulate the VGM effect is the green one (because the 30% of $S_{a,V}(T_z)$ is equal to 0.3g, see Table 5). From this result, it is clear that the cyclic hysteretic behavior is not significantly affected by the V component and the pushover analysis with permanently reduced gravity loads is too much conservative.

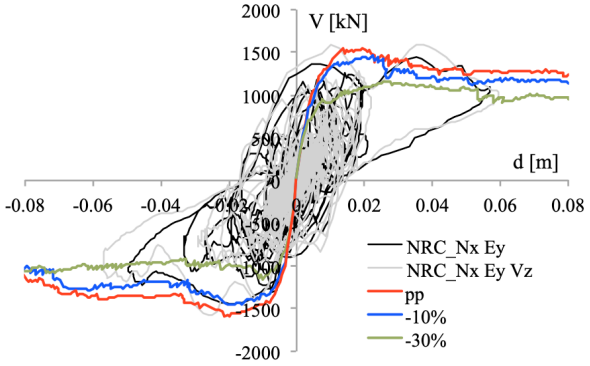

Fig. 7 – Comparison between the V-d response from NLDA with NRC record and pushover analysis from NLSA decreasing the vertical gravity forces

6. Conclusions and ongoing research

The paper presents the results of a preliminary study on the effect of the vertical ground motion component on the response of a case-study representative of an existing ordinary URM building. This topic is very hot at the moment, particularly in Italy after the earthquake in Central Italy in 2016. At present, the state-of-art is quite poor and a consolidated scientific literature does not exist yet. From these first analyses, a clear trend cannot be derived and the effect of the two components of the ground motion seems to play a role more significant than the three components. The maximum top displacement has been revealed for the examined case-study not to be an effective EDP, while more information can be obtained by analyzing the VGM effect at a *"local scale"*, for example considering the variation of the axial force for each step of the analysis or the damage pattern occurred in some selected piers. However, recent researches on URM case-studies [3] and past works on RC structures ([4], [5]) found out the incidence of the source-to-site distance on the vertical component effects. For this reason, the research is still ongoing and the Authors are performing NLDA on the same case-study with a relevant number of records, selected from the last Italian seismic events (2012 Emilian earthquake and 2016 Central Italy), considering different magnitudes, epicentral distances and seismic stations.

7. Acknowledgements

The activities are developed and are still ongoing within the national research project ReLUIS 2019-2021 (WP10 - Task 10.4) founded by the Italian Civil Protection Agency.

6. References

[1] Acito M, Bocciarelli M, Chesi C, Milani G (2014): Collapse of the clock tower in Finale Emilia after the May 2012 Emilia Romagna earthquake sequence: numerical insight. *Engineering Structures*, **74**,70-91.

[2] Comodini F, Fagotti G, Mezzi M (2019): Effects of the earthquake vertical components in masonry buildings: vertical collapse mechanisms?. *XVIII Convegno ANIDIS– L'Ingegneria Sismica in Italia*, Ascoli Piceno, Italy (in Italian).

[3] Di Michele F, Cantagallo C, Spacone E (2019): Effects of the vertical seismic component on seismic performance of an unreinforced masonry structures. *Bulletin of Earthquake Engineering*, https://doi.org/10.1007/s10518-019-00765-3.

[4] Kikuchi M, Dan K, Yashiro, K (2000): Seismic behavior of a reinforced concrete building due to large vertical ground motions in near-source regions. *12th World Conference on Earthquake Engineering*, Auckland, New Zealand.

[5] Diotallevi PP, Landi L (2000): Effect of the axial force and of the vertical ground motion component on the seismic response or R/C frames. *12th World Conference on Earthquake Engineering*, Auckland, New Zealand.

[6] Papazoglou AJ, Elnashai AS (1996): Analytical and field evidence of the damaging effect of vertical earthquake ground motion. *Earthquake Engineering & Structural Dynamics*, **25**, 1109-1137.

[7] Mwafy A, Elnashai AS (2006): Vulnerability of code-compliant RC buildings under multi-axial earthquake loading. *4th International Conference on Earthquake Engineering*, Taipei, Taiwan.

[8] Liberatore D, Doglioni C, AlShawa O, Atzori S, Sorrentino L (2019): Effects of coseismic ground vertical motion on masonry constructions damage during the 2016 Amatrice-Norcia (Central Italy) earthquakes. *Soil Dynamics & Earthquake Engineering*, 120, 423-435.

[9] Mariani M, Pugi F (2018): Effetti negativi del sisma verticale sul comportamento delle pareti esistenti in muratura. https://www.ingenio-web.it/20721-effettinegativi-del-sisma-verticale-sul-comportamento-delle-pareti-esistenti-in-muratura (in Italian).

[10] Mariani M, Pugi F (2019): La componente verticale è sempre da considerare perché rilevante vicino e lontano dalla sorgente. https://www.ingenio-web.it/25129-la-componente-sismica-verticale-e-sempre-da-considerare-perche-rilevante-vicino-e-lontano-dalla-sorgente (in Italian).

[11] Lagomarsino S, Penna A, Galasco A, Cattari S (2013): TREMURI program: an equivalent frame model for the nonlinear seismic analysis of masonry buildings. *Engineering Structures,* 56, 1787-1799.

[12] Mariani M, Francioso A, Pugi F (2018): Sisma verticale: amplificazione della vulnerabilità degli edifice esistenti in murtura. https://www.ingenio-web.it/21336-sisma-verticale-amplificazione-della-vulnerabilita-degli-edifici-esistenti-in-muratura (in Italian).

[13] Mariani M, Francioso A, Pugi F (2018): Sisma verticale: modellazione e analisi in ambito professionale sugli edifice esistenti in muratura. https://www.ingenio-web.it/22185-sisma-verticale-modellazione-e-analisi-in-ambito-professionale-sugli-edifici-esistenti-in-muratura (in Italian).

[14] Cattari S, Lagomarsino S (2013): Masonry Structures, pp. 151-200. *Developments in the field of displacement based seismic assessment*. Edited by T. Sullivan and G.M.Calvi, Ed. IUSS Press (PAVIA) and EUCENTRE.

[15] MIT (2019): Ministry of Infrastructures and Transportation, Circ. C.S.Ll.PP. No. 7 of 21/1/2019. Istruzioni per l'applicazione dell'aggiornamento delle norme tecniche per le costruzioni di cui al Decreto Ministeriale 17 Gennaio 2018. G.U. S.O. n.35 of 11/2/2019 (In Italian).

[16] Di Sarno L, Elnashai AS, Manfredi G (2011): Assessment of RC columns subjected to horizontal and vertical ground motions recorded during the 2009 L'Aquila (Italy) earthquake. *Engineering Structures,* 33, 1514-1535.

[17] Beyer K, Bommer JJ (2006): Relationship between median values and between aleaotory variabilities for different definitions of the horizontal component of motion. *Bulletin of Seismological Society of America*, 96, 1512-1522.

[18] Mann W, Muller H (1980): Failure of shear-stressed masonry – an enlarged theory, tests and application to shear-walls. *International Symposium on Load bearing Brickwork*, London, UK.

[19] Italian Technical Code (2018): Decreto Ministeriale 17/1/2018. Aggiornamento delle 'Norme tecniche per le costruzioni', Ministry of Infrastructure and Transportations. G.U. n.42 on 20/2/2018 (in Italian).

